The structural transformation and properties of spin-on poly(silsesquioxane) films by thermal curing

Wei-Chih Liu [a], Chang-Chung Yang [a], Wen-Chang Chen [a,*], Bao-Tong Dai [b], Ming-Shih Tsai [b]

[a] *Department of Chemical Engineering, National Taiwan University, Taipei 106, Taiwan*
[b] *National Nano Device Laboratories, National Science Council, Hsinchu 300, Taiwan*

Received 4 September 2001; received in revised form 11 March 2002

Abstract

In this study, the structural transformation and properties of five commercially available poly(silsesquioxanes) by thermal curing were investigated, including poly(hydrogen silsesquioxanes) (HSQ and T12), and poly(methyl-silsesquioxanes) (MSQ, T7 and T9). These materials with a different cage/network ratio and side groups (Si–H and Si–CH₃). The FTIR spectra show that the poly(silsesquioxane) films have different contents of the Si–O–Si cage and network structures, which significantly affects the refractive index and dielectric constant. The shifting of the Si–O–Si network band in the FTIR spectra can be correlated with their molecular structures. The refractive indices and dielectric constants of the studied poly(silsesquioxane) films increase with increasing the Si–O–Si network content. The retention of the Si–H or Si–CH₃ side group suggests the existence of the cage structures in the poly(silsesquioxane) films. The Si–O–Si cage structure results in a larger free volume than the Si–O–Si network structure in the poly(silsesquioxane) films and thus reduces the refractive index and dielectric constant. It is supported by the porosity result. The order of the refractive index in the studied poly(silsesquioxanes) films is T12 > HSQ for the Si–H side group and T7 > T9 > MSQ with the Si–CH₃ side group, which can be correlated with the Si–O–Si network content. The poly(silsesquioxane) film with the Si–CH₃ side group has a lower refractive index than the Si–H side group at the same Si–O–Si network content, which is probably due to the steric hindrance effect of the CH₃ group.
© 2002 Elsevier Science B.V. All rights reserved.

1. Introduction

Poly(silsesquioxanes) (POSS) such as hydrogen silsesquioxane (HSQ), methyl silsesquioxane (MSQ), and hydrido-organo siloxane polymer (HOSP) have been recognized as potential candidates for low dielectric constant materials [1–10]. The molecular structures of these materials consist a mixed cage/network structure before thermal curing. Part of the cage structures in these materials is transformed to a network structure after thermal curing. The structural modification in the above POSS materials by thermal curing results in a significant variation on their properties, including mechanical properties [11], and dielectric

---

properties [12,13], and refractive index [14,15]. Siew et al. studied the microstructures of HSQ in the temperature range of 350–450 °C [16]. They identified the possible Si–H thermal dissociation and the collapse of porous network by the thermogravimetric analysis (TGA) and the Fourier transform infrared (FTIR) spectrophotometer. They proposed four possible stages during curing of the HSQ film: (1) room temperature up to 200 °C: solvent loss; (2) 250–350 °C: network redistribution and SiO_2 formation; (3) 350–435 °C: Si–H thermal dissociation and cage–network redistribution; (4) >435 °C (or 450 °C): collapse of pore network. The cage/network structural transformation of HSQ by thermal curing has also been reported by Belot et al. [17], Loboda et al. [18], and Albrecht and Blanchette [19]. Our laboratories proposed a two-stage zero-order kinetics on the cage/network transformation on the HSQ films [14,15]. The cage structure of the HSQ film transforms into the network structure by thermal

curing and results in a significant change on the film properties such as refractive index and dielectric constant. For the POSS films with the Si–CH_3 group, Chua et al. [20] studied the curing behavior of MSQ in the temperature range of 350–500 °C. They found that the curing reaction of MSQ is an endothermic reaction accompanied by weight loss, shrinkage, and reduction in coefficients of thermal expansion and dielectric constant. Although there were several reports on the structures and properties of the POSS films by thermal curing, most of the above studies focused on one kind of the POSS films. The studies from Siew et al. [16] and our laboratories [14,15] have revealed the possible mechanism for the thermal curing of HSQ. However, a general structure–property relationship based on different kinds of POSS films by thermal curing has not been fully explored.

In order to investigate the structural transformation and properties of the POSS films by ther-
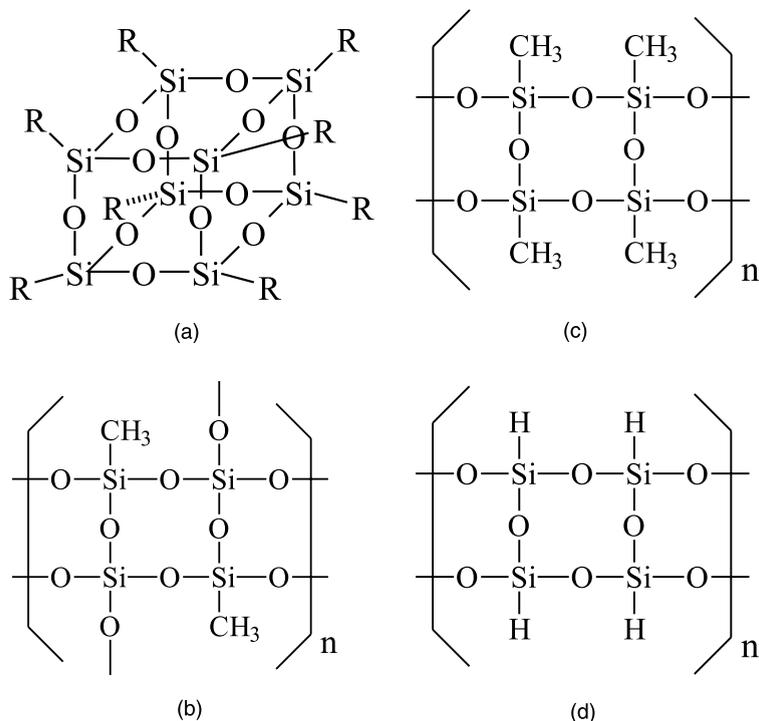

Fig. 1. The molecular structures of (a) R = H for HSQ, R = CH_3 for MSQ; (b) T7; (c) T9; (d) T12 for the studied poly(silsesquioxanes).

mal curing, five commercially available POSS films, poly(hydrogen silsesquioxanes) (HSQ and T12), poly(methylsilsesquioxanes) (MSQ, T7 and T9), were studied. The fundamental molecular structures of the studied POSS films are shown in Fig. 1, which include the cage form and the network form. HSQ and T12 are the materials with the Si–H side group while MSQ, T7, and T9 with the Si–CH$_3$ group. The correlations between the cage/network ratio, Si–H or Si–CH$_3$ residues, porosity, refractive index, and dielectric constant of the studied films were investigated.

2. Experimental

2.1. Materials and processing

HSQ (precursor: Fox 15), and MSQ (precursor: ACCUSPIN 418) were obtained from Dow Corning Corporation (Midland, MI, USA), and Honeywell Inc. (Sunnyvale, CA, USA) respectively. T7, T9, and T12 were purchased from Tokyo Ohka Kogyo (TOK) Co. (Tokyo, Japan). The studied five materials were spun coated on a 4 in. wafer by a spin-on glass (SOG) coater, and baked at different conditions according to Table 1.

2.2. Characterization

The chemical structure of the cured films on wafer was characterized by the FTIR. The transformation from the Si–O–Si cage structure to the total Si–O–Si structure (the cage structure + the network structure) was monitored through the variation of the peak area of the 1130 cm^{-1} peak and the 1000–1250 cm^{-1} peak. The refractive index and the film thickness of the cured films on wafer were then measured using a refractive index (n) and

extinction coefficient (k) analyzer which equipped with the light source of 190–900 nm wavelength. The analyzer detected the reflection of light from thin film and estimated the refractive index and thickness. The porosity (P) of the cured HSQ film was determined by the effective medium approximation (EMA) module of the ellipsometer. The dielectric constant of the HSQ film was obtained by a metal (Al)–insulator–metal (MIM) device. In this measurement, the capacitance of the MIM device was measured by C–V system. The dielectric constant (k) was then calculated from the following formula: $k = ct/A\varepsilon_0$, where c is the observed capacitance, t is the film thickness, A is the contacted area with the measured film, and ε_0 is the free permittivity. The experimental uncertainties of refractive index, thickness, and dielectric constant are ± 0.002, ± 3 nm, and ± 0.1, respectively.

3. Results

3.1. IR spectra

Fig. 2 shows the FTIR spectra of the studied POSS films after thermal curing. A broad Si–O–Si absorption band in the wave number range of 1000–1250 cm^{-1} is shown in all five spectra. It suggests the Si–O–Si backbone of the studied films. The absorption bands at 2258 and 830 cm^{-1} of Fig. 2(a) and (b) are resulted from the Si–H bond of the HSQ and T12. The Si–CH$_3$ absorption bands are found at 1273 and 768 cm^{-1} for MSQ, 1277 and 780 cm^{-1} for T7, and 1273 and 781 cm^{-1} for T9, respectively. The corresponding CH$_3$ absorption band appears around 2973 cm^{-1} for the films of MSQ, T7, and T9. There was no Si–OH absorption band around 3500 cm^{-1} in the spectra shown in Fig. 2, which shows the successful curing

Table 1
The conditions for preparing the studied POSS films

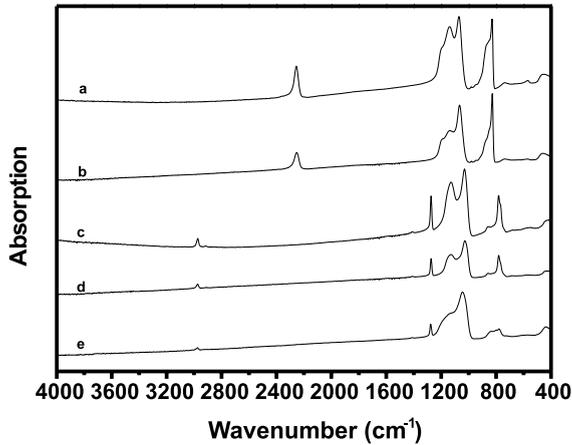| POSS	Processing	Curing conditions
HSQ	3000 rpm (20 s)	150 °C(1 min) → 200 °C(1 min) → 300 °C(1 min) → 400 °C(1 h, N$_2$)
T12	3000 rpm (20 s)	80 °C(1 min) → 150 °C(1 min) → 200 °C(1 min) → 400 °C(30 min, N$_2$)
MSQ	3000 rpm (20 s)	180 °C(1 min) → 180 °C(1 min) → 250 °C(1 min) → 400 °C(1 h, N$_2$)
T7	3000 rpm (20 s)	80 °C(1 min) → 150 °C(1 min) → 200 °C(1 min) → 400 °C(30 min, N$_2$)
T9	3000 rpm (20 s)	100 °C(1 min) → 180 °C(1 min) → 250 °C(1 min) → 400 °C(30 min, N$_2$)

Fig. 2. The FTIR spectra of the studied POSS films in the wave number range of 400–4000 cm^{-1}. (a) HSQ; (b) T12; (c) MSQ; (d) T9; (e) T7.

of the POSS films from their precursor solutions. An interesting feature for the FTIR spectra of the studied polymers is the splitting of the Si–O–Si absorption band into two bands around 1030–1070 and 1130 cm^{-1}, as shown in Fig. 3. These two bands can be assigned to the Si–O–Si network and Si–O–Si cage structures of the POSS films, respectively [14,15,18,19]. The absorption band of the Si–O–Si network structure is found at 1070 cm^{-1} in the spectra of HSQ and T12. By replacing
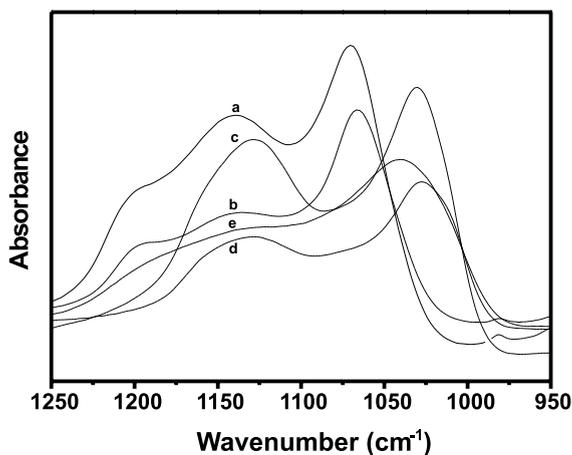

Fig. 3. The FTIR spectra of the studied POSS films in the wave number range of 950–1250 cm^{-1}. (a) HSQ; (b) T12; (c) MSQ; (d) T9; (e) T7.
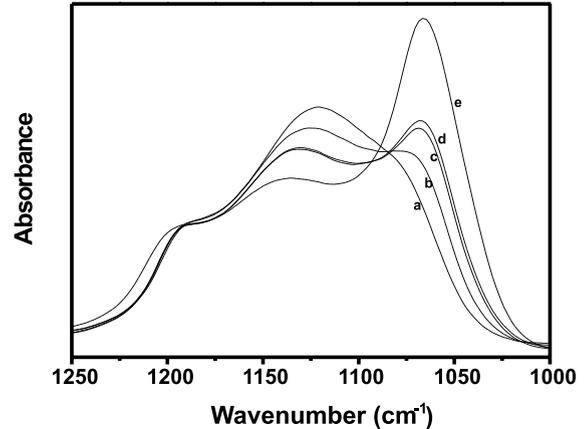

Fig. 4. The FTIR spectra of a typical HSQ film at different baking conditions in the wave number range of 1000–1250 cm^{-1}. (a) as spun-on; (b) 80 °C; (c) 150 °C; (d) 200 °C; (e) 400 °C.

the Si–H band with the Si–CH$_3$ band, the Si–O–Si network absorption band shifts to 1046 cm^{-1} of T7, and 1030 cm^{-1} of MSQ and T9. The FTIR study shows the prepared POSS films have the molecular composition of mixed cage and network structures. Fig. 4 shows the FTIR spectra of a typical HSQ film at different stages of curing temperature. The peak at 1130 cm^{-1} decreases with increasing curing temperature, which is assigned to the cage structure. However, the peak at 1070 cm^{-1} shows an opposite trend, which is assigned to the network structure. It suggests that the transformation of the cage/network structure is very sensitive to the curing temperature.

3.2. Structure–property relationships

In Fig. 5, the HSQ-1 to HSQ-5 mean that five different HSQ samples were baked in the furnace at 400 °C. However, it was found that the structure and properties of the cured HSQ samples show a significant variation because of the deviation of the furnace temperature. Fig. 5 shows the variation of the refractive indices of the five HSQ films with the FTIR peak ratios of the Si–O–Si network structure and the Si–H bond to the total Si–O–Si structure, respectively. The total Si–O–Si absorption band is in the wave number range of 1000–1250 cm^{-1},
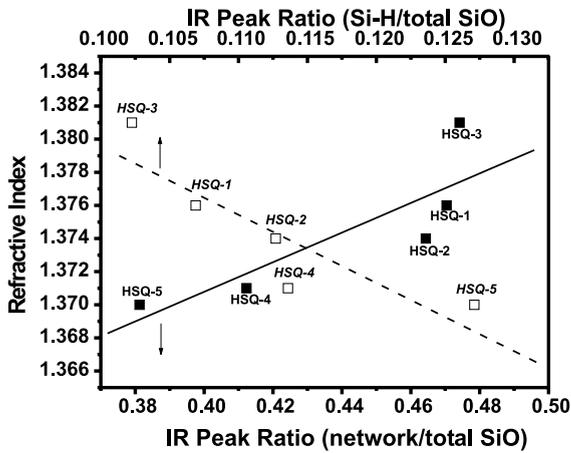
Fig. 5. Variation of the refractive index of five HSQ films with the FTIR peak ratio of the network Si–O–Si structure and the Si–H bond to the total Si–O–Si peaks, respectively.

which includes the absorption bands of the cage and network structures of the Si–O–Si bond. The refractive index of the studied HSQ films increases with increasing the ratio of the network structure but decreases with increasing the Si–H content in Fig. 5. Fig. 6 shows the variation of dielectric constant with the ratio of the network structure and the Si–H bond, respectively. This figure exhibits a similar trend as that of Fig. 5. It illustrates

the increasing of dielectric constant from 2.81 to 3.77 with increasing the content of the network structure and decreasing the Si–H bond in the cured HSQ films. In Figs. 7 and 8, it shows the porosity decreases from 16.5% to 12.3% with increasing the content of the network structure in the cured HSQ films and also illustrates the increase of the refractive index and dielectric constant of the HSQ films.

A similar observation on the structure and properties relationships is found on the cured poly(silsesquioxane) films with those of the HSQ films. The MSQ-1 $\sim$ 5, T7-1 $\sim$ 4, T9-1 $\sim$ 5, and

Fig. 7. Variation of porosity and refractive index of five HSQ films with the FTIR peak ratio of the network Si–O–Si structure to the total Si–O–Si peaks.
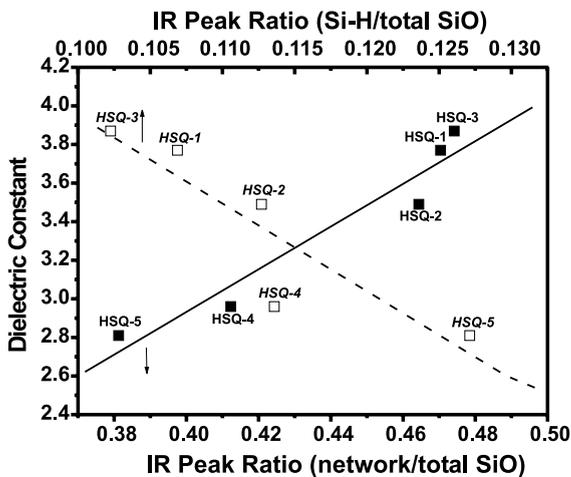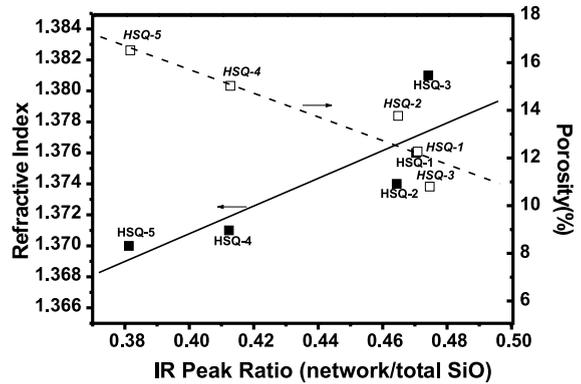

Fig. 6. Variation of the dielectric constant of five HSQ films with the FTIR peak ratio of the network Si–O–Si structure and the Si–H bond to the total Si–O–Si peaks, respectively.
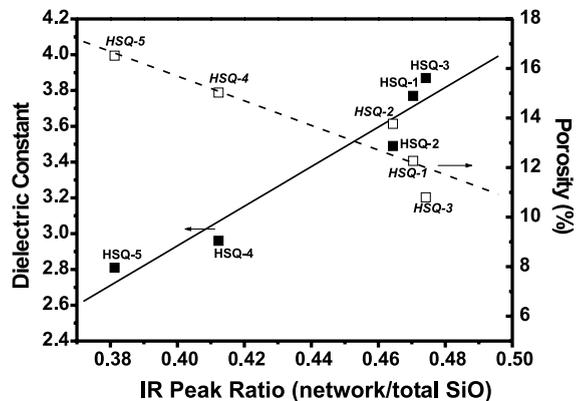

Fig. 8. Variation of porosity and dielectric constant of five HSQ films with the FTIR peak ratio of the network Si–O–Si structure to the total Si–O–Si peaks.
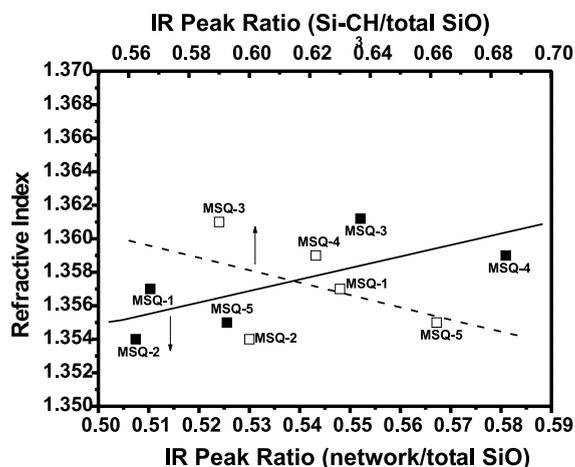
Fig. 9. Variation of refractive index of five MSQ films with the FTIR peak ratio of the network Si–O–Si structure and the Si–CH₃ bond to the total Si–O–Si peaks.

T12-1 ~ 5 mean cured poly(silsesquioxanes) due to the variation of furnace temperatures. Fig. 9 shows the variation of the refractive indices of the five MSQ films with the FTIR peak ratio of the Si–O–Si network structure and the Si–CH₃ bond to the total Si–O–Si structure. The refractive index increases from 1.354 to 1.361 as increasing the Si–O–Si network ratio and decreasing the Si–CH₃ ratio. The trend is similar to that of HSQ. How-
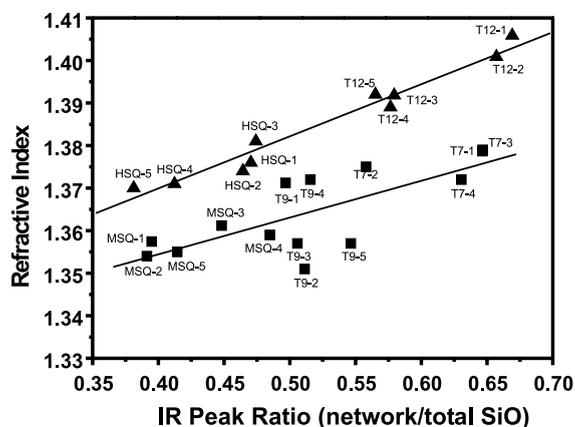

Fig. 10. Variation of refractive index of the studied HSQ, T12, MSQ, T7, and T9 films with the FTIR peak ratio of the network Si–O–Si structure to the total Si–O–Si peaks.

ever, the variation of the refractive index and the molecular structures is not as significant as the case of HSQ. Fig. 10 shows the variation of the refractive index of the cured POSS films with the FTIR peak ratio of the Si–O–Si network structure to the total Si–O–Si structure. For the studied POSS films, it has a general trend on the variation of the refractive index with the content of the network structure. That is, the refractive index increases with increasing the Si–O–Si network content. Furthermore, the order of the refractive index at the same Si–O–Si network ratio is T12 > HSQ > T7 > T9 > MSQ. The POSS films with the Si–CH₃ side group (T7, T9, MSQ) have a lower refractive index than the Si–H side group (HSQ, T12).

4. Discussion

4.1. Si–O–Si structure

In FTIR spectra, the Si–O–Si network absorption was shift to a lower wave number for the Si–CH₃ bond than that of the Si–H bond in the studied films. This is because the CH₃ group results in a steric hindrance of the molecular structure and thus decreases the polarization of Si–O–Si network structure. Furthermore, note that the CH₃ content of T7, T9, and MSQ are 11% and 20%, 22%, respectively. Therefore, the Si–O–Si network absorption of MSQ shifts to a lower wave number. The cage structure of the HSQ film is transformed to the network structure by thermal curing, as shown in Fig. 4, suggests that the transformation of the cage/network structure is very sensitive to the curing temperature. For the other poly(silsesquioxanes) in our study have the same tendency.

4.2. Structure–property relationship

For HSQ, the Si–H bond is very sensitive to the curing temperature. The bond cleavage of the Si–H bond results in the collapse of the cage structure and then the formation of the dense Si–O–Si network structure. The higher Si–H content suggests

the higher retention of the cage structure in the HSQ films. The cage structure results in a larger free volume of the molecular structure and thus results in a lower refractive index than the network structure. This result can be supported by the dielectric constant of the HSQ film. Since the dielectric constant is generally proportional to the refractive index, the results in Figs. 5 and 6 show the importance of the ratio of the cage/network structure on the properties of the HSQ films. The porosities of the five HSQ samples can further support the effects of the free volume for the ratio of the cage/network structure on the properties of the HSQ films. A similar observation on the structure and properties relationships is found on the MSQ films with those of the HSQ films. However, the variation of the refractive index and the molecular structures is not as significant as the case of HSQ. It suggests that the Si–CH_3 bond cleavage is not as thermal sensitive as the Si–H bond. The similar results could be found for the other poly(silsesquioxanes) in our study.

For the refractive index result of all poly(silsesquioxanes) in this study, the POSS films with the Si–CH_3 side group (T7, T9, MSQ) have a lower refractive index than the Si–H side group (HSQ, T12). It is probably because the materials with the CH_3 group results in a steric hindrance in the chemical structure, and thus has a larger free volume than the materials with the Si–H group. Furthermore, the Si–CH_3 content of T7, T9, and MSQ are 11%, 20%, and 22%, respectively. This explains the order of the refractive index shown in Fig. 10.

5. Conclusions

The structural transformation and properties of five commercially available POSS by thermal curing were studied. The POSS films by thermal curing have different Si–O–Si cage/network contents, which significantly affect the refractive index and dielectric constant. The refractive indices and dielectric constants of the studied POSS films decrease with increasing the Si–O–Si network content. It is supported by the porosity result. The order of the refractive index in the studied POSS

films is T12 > HSQ for the Si–H side group and T7 > T9 > MSQ with the Si–CH_3 side group, which can be correlated with the Si–O–Si network content. The POSS film with the Si–CH_3 side group has a lower refractive index than the Si–H side group at the same Si–O–Si network content, which is probably due to the steric hindrance effect of the CH_3 group.

Acknowledgements

References

[1] T.M. Lu, S.P. Murarka, T.S. Kuan, C.H. Ting (Eds.), Low-Dielectric Constant Materials-Synthesis and Applications in Microelectronics, Materials Research Society, Pittsburgh, PA, MRS. Symp. Proc., vol. 381, 1995.

[2] A. Lagendijk, H. Treichel, K.J. Uram, A.C. Jones (Eds.), Low-Dielectric constant Materials II, Materials Research Society, Pittsburgh, PA, MRS Symp. Proc., vol. 443, 1996.

[3] C. Case, P. Kohl, T. Kikkawa, W.W. Lee (Eds.), Low-Dielectric Constant Materials III, Materials Research Society, Pittsburgh, PA, MRS Symp. Proc., vol. 476, 1997.

[4] C. Chiang, P.S. Ho, T.M. Lu, J.T. Wetzel (Eds.), Low-Dielectric Constant Materials IV, Materials Research Society, Pittsburgh, PA, MRS Symp. Proc., vol. 511, 1998.

[5] J. Hummel, K. Endo, W.W. Lee, M. Mills, S.Q. Wang (Eds.), Low-Dielectric Constant Materials V, Materials Research Society, Pittsburgh, PA, MRS Symp. Proc., vol. 565, 1999.

[6] W.C. Chen, S.C. Lin, B.T. Dai, M.S. Tsai, J. Electrochem. Soc. 146 (1999) 3004.

[7] W.C. Chen, C.T. Yen, J. Polym. Res. 6 (1999) 197.

[8] W.C. Chen, C.T. Yen, J. Vac. Sci. Technol. B. 18 (2000) 201.

[9] M.J. Loboda, G.A. Toskey, Solid State Technol. 41 (1998) 99.

[10] J.N. Bremmer, Y. Liu, K.G. Gruszynski, F.C. Dall, in: C. Case, P. Kohl, T. Kikkawa, W.W. Lee (Eds.), Low-Dielectric Constant Materials III, Materials Research Society, Pittsburgh, PA, MRS Symp. Proc., vol. 476, 1997, p. 37.

[11] Y. Liu, F. Dall, in: J. Hummel, K. Endo, W.W. Lee, M. Mills, S.Q. Wang (Eds.), Low-Dielectric Constant Materials V, Materials Research Society, Pittsburgh, PA, MRS Symp. Proc., vol. 565, 1999, p. 267.

[12] H.C. Liou, J. Pretzer, Thin Solid Films 335 (1998) 186.

[13] R.F. Cook, E.G. Liniger, J. Electrochem. Soc. 146 (1999) 4439.

[14] C.C. Yang, W.C. Chen, L.M. Chen, C.J. Wang, Proc. Nsc. ROC. A 25 (2001) 339.

[15] C.C. Yang, W.C. Chen, J. Mater. Chem. 12 (2002) 1138.

[16] Y.K. Siew, G. Sarkar, X. Hu, A. See, C.T. Chua, J. Electrochem. Soc. 147 (2000) 335.

[17] V. Belot, R. Corriu, D. Leclercq, P.H. Mutin, A. Vioux, Chem. Mater. 3 (1991) 127.

[18] M.J. Loboda, C.M. Grove, R.F. Schneider, J. Electrochem. Soc. 145 (1998) 2861.

[19] M.G. Albrecht, C. Blanchette, J. Electrochem. Soc. 145 (1998) 4019.

[20] C.T. Chua, G. Sarkar, X. Hu, J. Electrochem. Soc. 145 (1998) 4007.